

First identification of the TiO $i^1\Pi$ - $a^1\Delta$ system in stellar spectra and its spectroscopic characterization[★]

Mirek R. Schmidt

Nicolaus Copernicus Astronomical Center, Polish Academy of Sciences, ul. Rabiańska 8, 87-100 Toruń, Poland
e-mail: schmidt@ncac.torun.pl

Received –, –

ABSTRACT

Context. TiO plays an important role in determining the atmospheric structure of M-type stars and in shaping the visual part of their spectra. The precision of synthetic spectra when confronted with high-resolution observations depends on the completeness of the included transitions and on the accuracy of line positions and line intensities.

Aims. We aim to systematically assess the quality of synthetic spectra computed with up-to-date TiO line lists by comparing them with high-resolution, high signal-to-noise spectra of cool stars calibrated in absolute or relative flux.

Methods. We compute synthetic spectra for late-type M giants and identify systematic discrepancies in the wavelength range 5810–5850 Å. To investigate the origin of these discrepancies, we analyse experimental TiO absorption cross-sections.

Results. We report the detection of a molecular band of the singlet system $i^1\Pi$ – $a^1\Delta$ of the TiO, with an R-head located at 5814.8 Å, overlapping the 1–3 band of the α ($C^3\Delta$ – $X^3\Delta$) system. The lower state of the band is identified as the $a^1\Delta v''=0$ state, while the upper state is most likely the $i^1\Pi$ in its ground vibrational state. The empirical band intensity is derived by comparing the relative strengths of neighbouring bands from the $C^3\Delta$ – $X^3\Delta$ and $B^3\Pi$ – $X^3\Delta$ systems in the experimental cross-section. The band intensity is further validated by synthetic spectrum calculations for the late-type giant 30 Her (M6 III) and comparison with its observed spectrum from the MELCHIORS library.

Conclusions. The $i^1\Pi$ (optionally $2^1\Pi$) electronic state has been predicted by theoretical calculations. While energies of two vibrationally excited states were previously inferred from de-perturbation analyses of the α system, accurate spectroscopic constants for this electronic state were lacking. The newly identified band is sufficiently strong to affect the flux distribution in the spectra of cool stars.

Key words. molecular data – stars: atmospheres – stars: late-type

1. Introduction

Since its identification in the spectra of M-type stars (Fowler 1904), TiO has been recognised as a major source of opacity in the atmospheres of cool stars. The visual spectra of late M-type stars are shaped by deep absorption features from electronic systems between low-lying states of TiO, providing key signatures for spectral classification (Merrill et al. 1962). In high-resolution spectra, TiO lines strongly affect synthetic spectra, and the analysis of weak atomic lines or other molecular bands is nearly impossible without prior identifying numerous TiO transitions (e.g. the determination of Li I; Woodward et al. 2020; Kamiński et al. 2023). At the same time, molecular bands, owing to the large number of states spanning a wide range of energies, provide valuable diagnostics of the dynamical behaviour of different layers in stellar atmospheres and their surroundings (see e.g. Tylenda et al. 2009).

To support stellar atmosphere modelling, line lists for TiO and its minor isotopologues were compiled (Jorgensen 1994; Plez 1998), initially based on laboratory measurements. As quantum-chemical *ab initio* calculations improved (Langhoff 1997), theoretically based line lists became available, including the AMES list (Schwenke 1998) and the more recent Toto list (McKemmish et al. 2019), produced within the ExoMol¹ effort

to determine molecular opacities in cool astrophysical objects (Tennyson et al. 2024).

A major advantage of *ab initio* methods is that they provide transition dipole moment functions, spin-orbit couplings, and other quantities required to compute band intensities, while also enabling physically motivated extrapolation to high vibrational and rotational levels (e.g. up to ($v=20$) and ($J=400$) in Toto) that contribute significantly to opacity at elevated temperatures.

Theory also allows estimates of the energies and properties of as yet unobserved states (see e.g. Dobrodey 2001; Miliordos & Mavridis 2010) and of bands that may be too weak in normal giants but detectable under specific astrophysical conditions. For example, the Schwenke (1998) line list includes the forbidden $c^1\Phi$ – $X^3\Delta$ and $b^1\Pi$ – $X^3\Delta$ bands, later identified in the spectrum of the red nova V838 Mon during the cooling phase after its eruption (Kamiński et al. 2009).

Despite these advances, theoretical calculations still do not provide sufficiently accurate line positions, so *ab initio* line lists rely heavily on precise laboratory data. Since its astronomical identification, TiO has been extensively studied in the laboratory and is now among the best-characterised transition-metal oxides (Merer 1989; see e.g. Phillips 1973; Ram et al. 1999; Barnes et al. 1997, summarized by McKemmish et al. 2017). More recent work includes analyses of singlet transitions by Bernath's group (Hodges & Bernath 2018; Bittner & Bernath 2018) and the weak ϵ band (Bernath & Cameron 2020).

[★] Full Tables 1 and 3 are only available at the CDS.

¹ www.exomol.com

A recent study of the TiO γ' ($B^3\Pi-X^3\Delta$) system by Bernath et al. (2025) analysed the ($\Delta v=+1$) sequence and derived spectroscopic constants for vibrationally excited levels of the $B^3\Pi$ state up to ($v=4$). Using spectra of a late-type giant and a dwarf, they demonstrated the high accuracy achievable with high-quality data, although fitting the absolute flux distribution required modifications to the intensities of excited bands relative to those adopted from the Toro line list. For such *ad hoc* adjustments to be reliable, they should be physically justified. The present work is motivated by a systematic verification of available molecular line lists in both line positions and band intensities.

Here we focus on the spectral region blueward of the $B^3\Pi-X^3\Delta$ (1–0) system, dominated by TiO lines overlapping with the excited $C^3\Delta-X^3\Delta$ ($\Delta v=-2$) sequence. We identify and analyse in detail a band of the previously unknown singlet system $i^1\Pi-a^1\Delta$. Section 2 presents the experimental and observational data. The observational motivation and analysis of the band, search for other bands of the system are given in Sect. 3. In section 3 we discuss also the application of the resulting line list to stellar spectra and the empirical determination of line strengths. Section 4 provides a broader discussion and Sect. 5 presents final remarks.

2. Spectral data

The experimental TiO cross-section used in this analysis was described in detail and made publicly available by Bernath (2020). It is based on an emission spectrum recorded in 1985 at the McMath–Pierce Solar Telescope using the 1 m Fourier transform spectrometer operated by the National Solar Observatory at Kitt Peak, Arizona, by S. Davis, G. Stark, J. Wagner, and R. Hubbard. The excitation temperature of the gas was determined to be (2300 ± 100) K by simulating the (0–0) band of the $A^3\Phi-X^3\Delta$ transition with PGOPHER (Western 2017) using the spectroscopic constants of Ram et al. (1999). The spectral resolution is 0.044 cm^{-1} , and the wavenumber scale was calibrated to an accuracy of $\pm 0.002\text{ cm}^{-1}$ (see Bernath 2020 for details). This is the same experimental spectrum used in a series of previous TiO studies (Bernath et al. 2025; Cameron & Bernath 2022; Bernath & Cameron 2020). In the following, we refer to this dataset simply as the experimental spectrum, unless stated otherwise. A portion of the experimental cross-section is shown as a solid black line in Fig. 1.

For the analysis of stellar spectra, we used data from the MELCHIORS library (Royer et al. 2024), a spectral survey of bright northern-hemisphere stars. The spectra were obtained with the HERMES spectrograph (Raskin et al. 2011) mounted on the Mercator Telescope at the Roque de los Muchachos Observatory on La Palma, Spain. The library provides high spectral resolution ($(R \approx 85,000)$) and high signal-to-noise ratios, with spectra corrected for the instrumental response and preserving the relative spectral energy distribution. This also applies to the spectrum of 30 Her (M6 III) used in this work. Its signal-to-noise ratio in the visual range is about 97, which is sufficient for our analysis.

3. Method and results

The direct motivation for searching for a new band was the observation of extra opacity in the spectra of late-type giants within a spectral region that almost exactly coincides with the α ($C^3\Delta-X^3\Delta$) (1–3) band, which extends redward from its band head

at 5809.9 \AA . This discrepancy becomes evident when synthetic spectra are compared with observations. An example is shown in Fig. 2 for the MELCHIORS spectrum of the late-type giant 30 Her (M6 III).

The synthetic spectrum calculated with an available list of lines is above the flux in the observed spectrum. Details of the fitting procedure are discussed in text below.

The mismatch cannot be explained by adjusting the relative intensities of the $C^3\Delta-X^3\Delta$ (0–2) and (1–3) bands. Even with modified band strengths, the synthetic spectrum fails to reproduce the fine structure of the observations. Similar results were obtained for other late-type giants. In contrast, when the stellar spectrum was overplotted with the experimental TiO spectrum, nearly all features in this wavelength region showed close correspondence. This strongly suggested that the missing opacity originates from a TiO band that is poorly represented or absent in existing line lists.

The stellar spectrum alone provides only the position of the apparent band head of the unknown system, measured at $(5814.8 \pm 0.1)\text{ \AA}$ or $(17,192.73 \pm 0.3)\text{ cm}^{-1}$.²

3.1. Analysis of the laboratory spectrum

The laboratory spectrum was analysed using the molecular spectroscopy fitting program PGOPHER (Western 2017). The overlapping bands of the α system were simulated using spectroscopic constants from Hedges & Bernath (2018). To reproduce line positions accurately at high J , small adjustments to the spectroscopic constants of the $C^3\Delta$ $v=0$ and $v=1$ states were required; only the higher-order correction terms (A_H) were modified.

A detailed inspection of the laboratory spectrum revealed several relatively strong unassigned line pairs exhibiting characteristic Δ -splitting, later identified as Q(e/f)-branch transitions. Subsequent analysis uncovered sequences belonging to the P and R branches of both parities. The Q-branch lines are approximately twice as strong as those of the P and R branches, and the observed line splittings indicated that the system involves a Π state. The stellar position of the band head provided a constraint on the location of the R head, which is not clearly distinguished in the laboratory spectrum.

After several iterations of assigning rotational quantum numbers J to individual lines, and allowing spectroscopic parameters of both the upper and lower states to vary simultaneously, a satisfactory fit was obtained. In total, 161 transitions assigned to the investigated band were fitted using the N^2 Hamiltonian, covering J from 7 to 54 in the P branch, J from 21 to 69 in the R branch, and J from 10 to 77 in the Q branch. The standard deviation of the fit is 0.018 cm^{-1} . The resulting spectroscopic parameters are listed in Table 2. The absolute energy of the $a^1\Delta$ state was fixed at the value derived from analysis of the forbidden $C^3\Delta-a^1\Delta$ system (Kaledin et al. 1995). A detailed list of fitted transitions is given in Table 1.

Allowing the lower-state parameters to vary led to two possible solutions. The preferred solution identifies the lower state as $a^1\Delta$, as presented in Table 2. An alternative solution involved the $X^3\Delta$, $\Omega = 3$ spin component (Ram et al. 1999). This possibility was excluded based on the astrophysical arguments discussed in Sect. 4.

The spectroscopic parameters of the upper state do not match those of any previously well-characterised electronic state, either in band origin or rotational constant. We therefore conclude

² Wavelengths are given in air, and wavenumbers in vacuum.

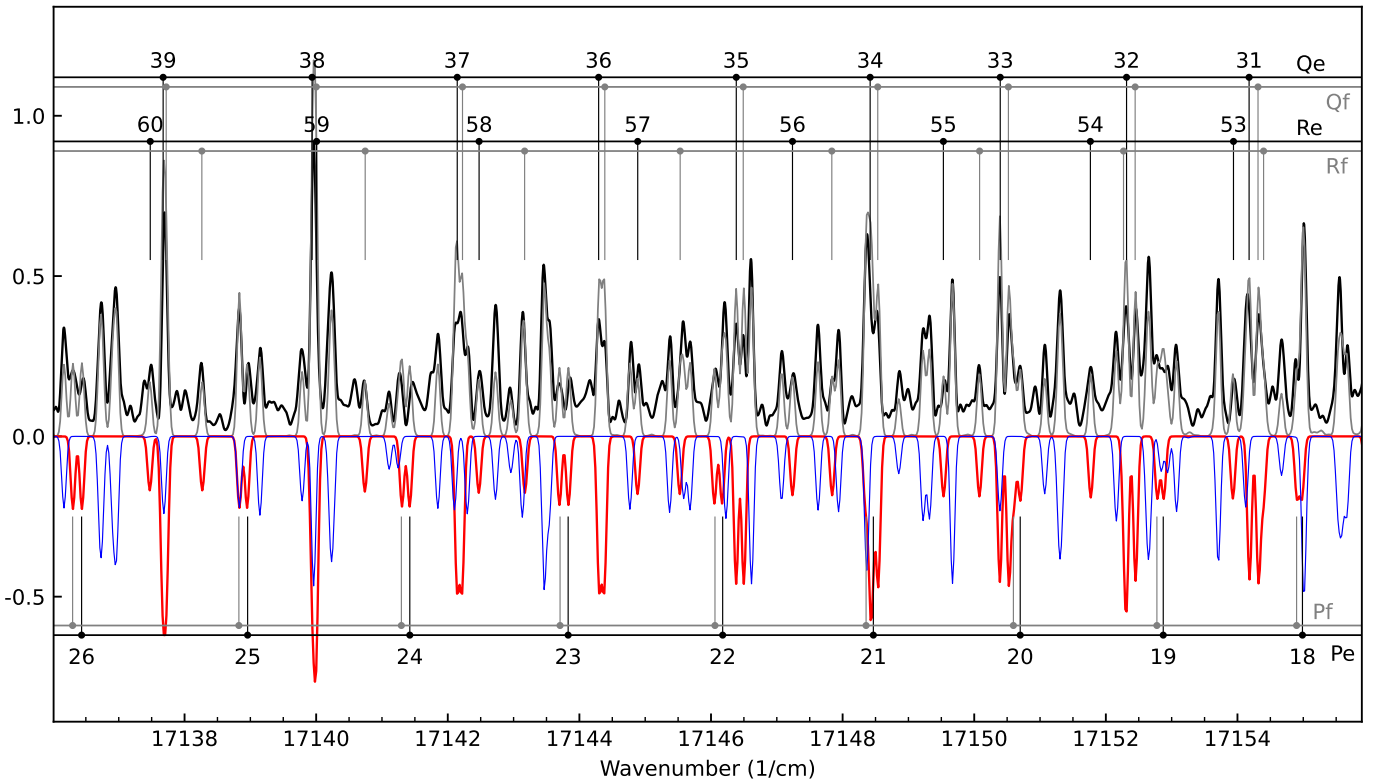


Fig. 1: Detailed view of the laboratory spectrum showing features of the $i^1\Pi - a^1\Delta$ (0-0) band. The laboratory spectrum is plotted in black, with the full simulated spectrum overplotted in grey. The mirrored spectra illustrate the separate contributions of the $C^3\Delta - X^3\Delta$ (0-2) and (1-3) bands (blue) and the $i^1\Pi - a^1\Delta$ (0-0) band (red). Line assignments for individual transitions of the $i^1\Pi - a^1\Delta$ band in the P, Q, and R branches, for both parities, are indicated above and below the spectrum. The rotational quantum numbers J apply to both parities.

Table 1: Sample of lines and residuals for the analysed band.

J'	e/f'	J''	e/f''	Observed (cm^{-1})	Calculated (cm^{-1})	Obs - Calc (cm^{-1})	Line Assignment
41	f	41	e	17132.9805	17132.9768	0.0037	qQe(41) $i^1\Pi v=0 41 41 F1f - a^1\Delta v=0 41 41 F1e$
41	e	41	f	17132.9805	17132.9816	-0.0011	qQf(41) $i^1\Pi v=0 41 41 F1e - a^1\Delta v=0 41 41 F1f$
63	f	62	f	17133.1052	17133.1196	-0.0144	rRf(62) $i^1\Pi v=0 63 63 F1f - a^1\Delta v=0 62 62 F1f$
26	e	27	e	17133.8847	17133.8544	0.0303	pPe(27) $i^1\Pi v=0 26 26 F1e - a^1\Delta v=0 27 27 F1e$
62	e	61	e	17134.8949	17134.8928	0.0021	rRe(61) $i^1\Pi v=0 62 62 F1e - a^1\Delta v=0 61 61 F1e$
40	f	40	e	17135.3640	17135.3543	0.0097	qQe(40) $i^1\Pi v=0 40 40 F1f - a^1\Delta v=0 40 40 F1e$
40	e	40	f	17135.3640	17135.3809	-0.0169	qQf(40) $i^1\Pi v=0 40 40 F1e - a^1\Delta v=0 40 40 F1f$
25	f	26	f	17136.3032	17136.2990	0.0042	pPf(26) $i^1\Pi v=0 25 25 F1f - a^1\Delta v=0 26 26 F1f$
25	e	26	e	17136.4604	17136.4355	0.0249	pPe(26) $i^1\Pi v=0 25 25 F1e - a^1\Delta v=0 26 26 F1e$
61	e	60	e	17137.4918	17137.4788	0.0130	rRe(60) $i^1\Pi v=0 61 61 F1e - a^1\Delta v=0 60 60 F1e$
39	f	39	e	17137.6973	17137.6746	0.0227	qQe(39) $i^1\Pi v=0 39 39 F1f - a^1\Delta v=0 39 39 F1e$
39	e	39	f	17137.6973	17137.7210	-0.0237	qQf(39) $i^1\Pi v=0 39 39 F1e - a^1\Delta v=0 39 39 F1f$
61	f	60	f	17138.2531	17138.2628	-0.0097	rRf(60) $i^1\Pi v=0 61 61 F1f - a^1\Delta v=0 60 60 F1f$

Notes. The line assignment illustrate the transition ${}^{\Delta N} \Delta J(e/f'')(J'') i^1\Pi v' J' N' F1p' - a^1\Delta^+ v'' J'' N'' F1p''$. The full table is available at the CDS.

that the observed band belongs to a previously unrecognised singlet system, $^1\Pi - a^1\Delta$. Following the convention adopted in the Toro/ExoMol TiO line list (McKemmish et al. 2019), we designate the upper state as $i^1\Pi$. We further assume that the upper state is the $v=0$ vibrational level. The justification for this assumption is given in Sect. 4.

In fact, the upper $i^1\Pi$ state is not entirely unknown. vibrationally excited levels of this state were reported by Namiki et al. (2003) in their study of perturbations affecting excited $C^3\Delta$ levels observed in α -system bands, based on laboratory data from Phillips (1973). They derived spectroscopic parameters for two consecutive vibrational levels of the perturbing state, although their absolute vibrational numbering remained uncertain.

Table 2: Spectroscopic constants for the $i^1\Pi$ and $a^1\Delta$ $v=0$ states of TiO.

	$i^1\Pi$ $v=0$	$a^1\Delta$ $v=0$ (this work)	Bittner & Bernath (2018)	Amiot et al. (1996)
T_v	20627.5192(38)	3444.367 ^a		
B_v	0.507108(60)	0.536255(61)	0.53624855(795)	0.5362187(24)
$D_v \times 10^7$	6.07(11)	6.13(11)	6.0293(115)	5.9914(24)
$H_v \times 10^{10}$				
$q \times 10^4$	3.683(85)			
$q_D \times 10^7$	-2.625(58)			
$q_H \times 10^{11}$	2.916(91)			

Notes. All values are in cm^{-1} . One standard deviation error is indicated in parentheses. ^(a) Parameter held fixed in the fit at value derived by Kaledin et al. (1995)

With the adopted identification of the observed level as the $v=0$ state of $i^1\Pi$, we assign Namiki et al. (2003) levels to $v=2$ and $v=3$. As noted by Namiki et al. (2003), the $v=3$ level exhibits irregular behaviour, with an increasing rotational constant B_v , which they attributed to interaction with the as yet unobserved $h^1\Sigma^+$ state. Their value for the $v=2$ rotational constant, $B_v = 0.5018 \pm 0.0044 \text{ cm}^{-1}$ (their Table 5), can be directly compared with the value derived here. Assuming $\alpha_e = 3 \times 10^{-3} \text{ cm}^{-1}$, typical for TiO electronic states to within about 10% (see Table 5 of Miliordos & Mavridis 2010), and using relation $B_v = B_e - \alpha_e(v + 1/2)$ to derive $B_e = 0.508608 \text{ cm}^{-1}$ from B_v for $v=0$, we obtain $B_v = 0.501108 \text{ cm}^{-1}$ for $v=2$, in agreement within uncertainties with the value of Namiki et al. (2003).

Figure 1 shows a portion of the laboratory spectrum together with PGOPHER simulations of the $i^1\Pi - a^1\Delta$ (0–0) band and the overlapping $C^3\Delta - X^3\Delta$ bands. The displayed region contains the strongest lines of the $i^1\Pi - a^1\Delta$ system.

The sign of the q parameter was determined using the pure precession and unique perturber approximations, in which the Δ -doubling parameter of a state of energy E perturbed by a state at energy E_{pert} is approximated by

$$q = \frac{4B^2}{E - E_{\text{pert}}} \quad (1)$$

where B is the rotational constant of the perturbed state (Lefebvre-Brion & Field 1985). Applying this relation to the $b^1\Pi$ and $i^1\Pi$ states allows an estimate of the energy of the perturbing state. Using $T(v=0)$, q , and B for $b^1\Pi$ ($14\,716 \text{ cm}^{-1}$, -1.6325×10^{-4} , and $0.51204209 \text{ cm}^{-1}$, respectively (Bittner & Bernath 2018) and the corresponding parameters for $i^1\Pi$ from Table 2, we derive an estimated perturber energy of $18\,812 \text{ cm}^{-1}$.

This is consistent with theoretical predictions for the unobserved singlet state $h^1\Sigma^+$: Miliordos & Mavridis (2010) obtained $T_e = 18\,596 \text{ cm}^{-1}$ at the MRCI+Q level (their state $2^1\Sigma^+$), while Schwenke (1998) reported $T_e = 17\,564.88 \text{ cm}^{-1}$. The perturbed states and the perturber differ mainly by $\pi\delta$ versus δ^2 configurations (Schwenke 1998; Merer et al. 1987), satisfying the assumptions of the approximation. This analysis supports the adopted assignment of e and f parities.

The laboratory position of the R head of the $i^1\Pi - a^1\Delta$ (0–0) band corresponds to the interpolated position of the $R_e(17)$ line at $17\,192.524 \text{ cm}^{-1}$ (5814.88 \AA), while the Q branch begins with $Q_f(2)$ at $17\,182.979 \text{ cm}^{-1}$ (5818.10 \AA).

3.2. Search for other bands

Encouraged by the successful analysis of the (0–0) band we searched for the next band in the $\Delta v=0$ sequence.

To this end, we estimated the vibrational constants ω_e (and $\omega_e x_e$) using the band origins derived in this work together with those reported by Namiki et al. (2003). A linear fit to the origins of the $v=0$, 2, and 3 levels gives $\omega_e = 841 \text{ cm}^{-1}$. Including the anharmonic term in the expansion does not change the result, as the derived $\omega_e x_e$ is close to zero. Fixing the anharmonic term at a value typical for other electronic states, $\omega_e x_e = 4 \text{ cm}^{-1}$, yields $\omega_e = 857 \text{ cm}^{-1}$.

Theoretical calculations by Miliordos & Mavridis (2010) give $\omega_e = 924 \text{ cm}^{-1}$ and $\omega_e x_e = 4 \text{ cm}^{-1}$.

One may also estimate ω_e using the approximate formula (exact for a Morse potential)

$$D_v = \frac{4B^3}{\omega_e^2} \quad (2)$$

This yields $\omega_e = 933 \text{ cm}^{-1}$ with an uncertainty of about 15 cm^{-1} , arising from the uncertainty in D_v . Overall, the value of ω_e remains poorly constrained.

These estimates allowed us to narrow the search range for the $i^1\Pi - a^1\Delta$ bands (1–1) and (1–0) in the experimental spectrum. In particular, we searched for characteristic patterns formed by Q-branch lines ($J=38\text{--}41$), where the expected Δ -doubling is close to zero and lines of both parities overlap, forming features of approximately twice the usual intensity. So far, however, we have been unable to reliably identify lines belonging to the (1–1) or (1–0) bands. Therefore the value of ω_e remains uncertain.

The identification of lines belonging to the (0–1) and (0–2) bands in the laboratory spectrum was also unsuccessful, despite their positions being well constrained using spectroscopic parameters of excited levels of $a^1\Delta$ from Bittner & Bernath (2018). The R-head positions of the (0–1) and (0–2) bands are expected at 6177.116 \AA ($R_e(19)$, $16\,184.307 \text{ cm}^{-1}$) and 6583.435 \AA ($R_e(21)$, $15\,185.329 \text{ cm}^{-1}$), respectively. The (0–1) band lies in the crowded region of the $B^3\Pi - X^3\Delta$ (0–0) band.

Because the experimental spectrum represents an absorption cross-section at an excitation temperature of 2300 K, the populations of the $a^1\Delta$ $v=1$ and $v=2$ levels are reduced by factors of approximately 2 and 4, respectively, relative to $v=0$, further decreasing the chances of their identification.

3.3. Empirical intensities

The empirical intensities of lines in the $i^1\Pi - a^1\Delta$ 0–0 band were determined in two ways. First, we estimated the

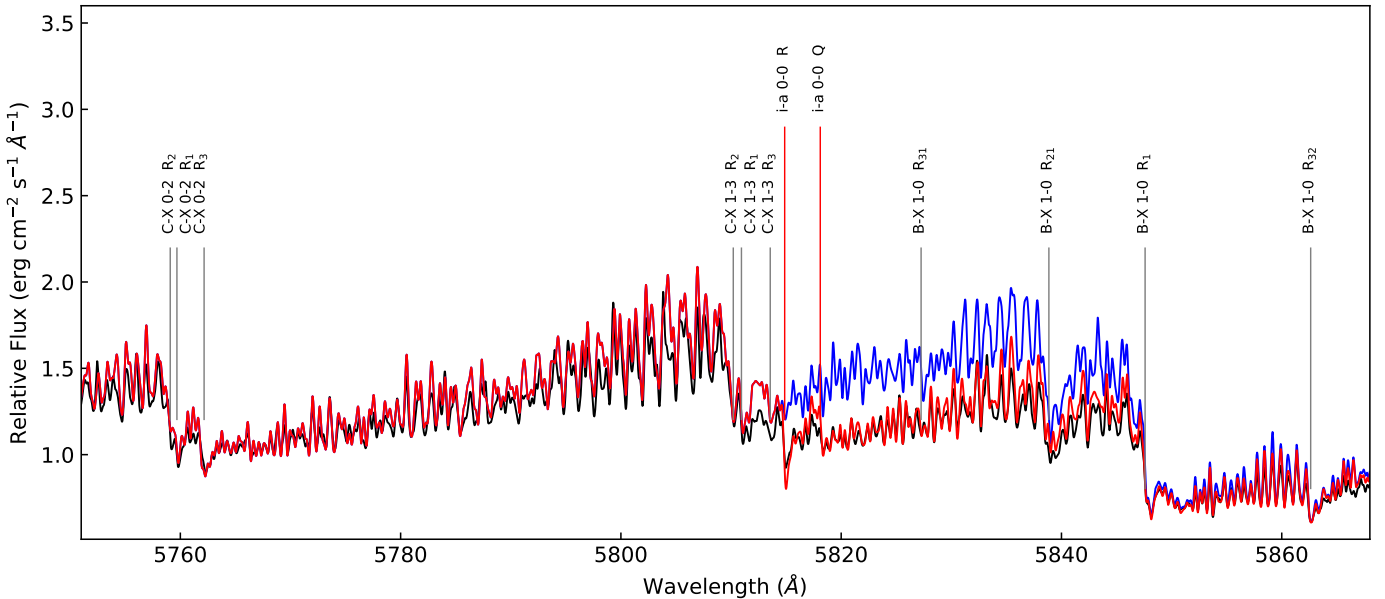


Fig. 2: MELCHIORS spectrum of 30 Her (black) with over-plotted synthetic spectra calculated for updated Toro list of lines described in text without (blue) and with (red) lines of the $i^1\Pi - a^1\Delta$ (0–0) band

band strength from simulations of the experimental cross-section performed with PGOPHER. The spectroscopic constants for the $C^3\Delta - X^3\Delta$ (0–2) and (1–3) bands were taken from Hodges & Bernath (2018). The $B - X$ bands were simulated using data from Cameron & Bernath (2022) and Bernath et al. (2025). The strength parameter for each simulated band in PGOPHER was fixed to reproduce oscillator strengths from the Toro line list (McKemmish et al. 2019). With this approach, the relative strengths of rotational lines within each band follow the Hönl–London factors calculated by PGOPHER from effective Hamiltonians.

The strength parameter of the $i^1\Pi - a^1\Delta$ band was then adjusted to match the laboratory spectrum, and oscillator strengths of individual lines were derived. The resulting spectrum, together with individual contributions of overlapping bands, is shown in Fig. 1. In the simulations, the excitation temperature was fixed at 2300 K, and individual lines were broadened with a Gaussian profile of width 0.078 cm^{-1} .

In the next step, we calculated a synthetic spectrum of a late-type giant. For this purpose, we used a TiO line list (including isotopologues) based on the Toro line list (McKemmish et al. 2017, 2019). The list was modified by replacing lines of selected bands of the γ' system with those from the recent analysis of Bernath et al. (2025). Only bands with $v', v'' \leq 6$ were replaced.³

This list was extended with the $i^1\Pi - a^1\Delta$ line list for the main isotopologue and corresponding lines of minor Ti isotopes. Isotopic corrections were adopted from McKemmish et al. (2017), as implemented in the Toro list. The isotopic shifts were derived from their $i^1\Pi$ and $a^1\Delta$ states. Although the $i^1\Pi$ energies calculated by McKemmish et al. (2017) are higher than the observed values reported here, their effect on the isotopic corrections was neglected.

As a model atmosphere for 30 Her, we adopted a MARCS model with standard chemical composition, solar metallicity,

$T_{\text{eff}} = 3000 \text{ K}$, $\log g = 0.5$, and $v_t = 4 \text{ km s}^{-1}$ (Gustafsson et al. 2008). The adopted temperature is somewhat lower than expected for an M6 III star. The primary motivation for this choice was to achieve the best simultaneous fit to neighbouring bands. Using higher T_{eff} values makes it difficult to reproduce both the α and γ' systems simultaneously with the adopted line list.

We find that no additional adjustment of the $i^1\Pi - a^1\Delta$ band strength is required to reproduce the spectrum of the giant. The results of the analysis are illustrated by the synthetic spectrum overplotted on the MELCHIORS spectrum of 30 Her in Fig. 2. Inclusion of the $i - a$ band fills the previously missing opacity without requiring any modification of the intensity of the $C^3\Delta - X^3\Delta$ (1–3) band.

An underestimation of opacity in a narrow range around 5812 Å remains unexplained. This position coincides with one of the heads of the $\text{ScO} A^2\Pi - X^2\Sigma^+$ (1–0) band, but its predicted intensity is insufficient to account for the discrepancy. Some mismatches in the region blueward of the $B^3\Pi - X^3\Delta$ (1–0) R_{21} head of the satellite band may be due to the unanalysed (1–1) band of the $i^1\Pi - a^1\Delta$ system. The contribution of the $\text{VO} C^4\Sigma - X^4\Sigma$ (1–1) band near 5786 Å was neglected in this figure.

The accuracy of the derived line strengths is estimated to be uncertain by up to 15%. Because the potential energy curve of the upper state is not known, the Franck–Condon factors cannot be determined independently. The oscillator strength of the (0–0) band derived from the fit is $f_{00} = 0.082$. The non-detection of the (0–1) and (0–2) bands provides upper limits on their strengths of $f_{01} \leq 0.09$ and $f_{02} \leq 0.09$.

The empirical line list for the $i^1\Pi - a^1\Delta$ (0–0) band of the main isotopologue $^{48}\text{Ti}^{16}\text{O}$, based on the derived spectroscopic constants and empirical intensities extrapolated up to $J=200$, is available as supplementary material. A sample of the list with abbreviated line assignments is shown in Table 3.

4. Discussion

The next $^1\Pi$ electronic state of TiO above $b^1\Pi$ was predicted several decades ago (see the summary by Merer 1989).

³ Because vibrational and spin quantum numbers show some non-monotonic behaviour for $J > 100$, it was first necessary to modify state assignments for the upper and lower levels in the original states file; see Yurchenko et al. (2016) for discussion of this issue.

Table 3: Sample table for the PGOPHER line list for the $i^1\Pi - a^1\Delta$ transition of TiO.

J'	P'	J''	P''	Position (cm $^{-1}$)	E_{up} (cm $^{-1}$)	E_{low} (cm $^{-1}$)	A (s $^{-1}$)	f	Line Assignment
63	e	62	e	17132.249	22661.877	5529.628	3785791.4	0.0196	rRe(62) : $i^1\Pi$ v=0 63 63 F1e - $a^1\Delta$..
41	f	41	e	17132.977	21498.958	4365.981	8000738.8	0.0409	qQe(41) : $i^1\Pi$ v=0 41 41 F1f - $a^1\Delta$..
41	e	41	f	17132.982	21498.963	4365.981	8000745.5	0.0409	qQf(41) : $i^1\Pi$ v=0 41 41 F1e - $a^1\Delta$..
63	f	62	f	17133.120	22662.747	5529.628	3786368.7	0.0196	rRf(62) : $i^1\Pi$ v=0 63 63 F1f - $a^1\Delta$..
26	f	27	f	17133.715	20983.141	3849.426	4545768.7	0.0224	pPf(27) : $i^1\Pi$ v=0 26 26 F1f - $a^1\Delta$..
26	e	27	e	17133.854	20983.280	3849.426	4545879.5	0.0224	pPe(27) : $i^1\Pi$ v=0 26 26 F1e - $a^1\Delta$..

Notes. J is the total angular momentum, P is the rotationless parity, Position is the calculated line position in cm $^{-1}$, E_{up} and E_{low} are the upper and lower energy levels in cm $^{-1}$, A is the Einstein $A_{J' \leftarrow J''}$ value in s $^{-1}$, and $f_{J' \leftarrow J''}$ is the oscillator strength, and line assignments are the associated quantum numbers for the given transition. The line assignment illustrate the transition ${}^{\Delta N} \Delta J(e/f)''(J'') : i^1\Pi v' J' N' F1p' - a^1\Delta v'' J'' N'' F1p''$. The full table is available at the CDS.

Quantum-chemical *ab initio* calculations have since provided estimates of its energy (Dobrodey 2001; Miliordos & Mavridis 2010). The value closest to that derived in this work is that of Miliordos & Mavridis (2010), who obtained $T_e = 21,100$ cm $^{-1}$ for the $i^1\Pi$ (their $2^1\Pi$) state at the MRCI+Q level of theory. Based on these calculations, we infer that the observed upper state is in its ground vibrational mode.

The transition dipole moment of the $i^1\Pi - a^1\Delta$ system was estimated by Dobrodey (2001), who obtained a value of 0.9 a.u. near the equilibrium internuclear distance (3.1 a.u.) (see their Figure 8). However, the predicted energy for the $i^1\Pi$ state was 27 052 cm $^{-1}$ significantly higher than the 20 627 cm $^{-1}$ determined here. Using their theoretical transition energy ($\nu_{vv'} = 23600$ cm $^{-1}$), this corresponds to an oscillator strength of $f_{00} = 0.036$ (see Eq. 1 of Dobrodey 2001).

The identification of the $i^1\Pi - a^1\Delta$ band increases the number of rotationally analysed singlet states of TiO to seven. The $i^1\Pi$ state was the last low-lying singlet state of the $\delta\pi$ configuration with previously undetermined energy (Merer et al. 1987; Merer 1989), alongside $A^3\Phi$, $B^3\Pi$, and $c^1\Phi$.

When the presence of the unidentified band of TiO was first confirmed in stellar spectra, plausible candidates included forbidden bands of the $D^3\Sigma^- - X^3\Delta$ (5–0 or 6–0) and $h^1\Sigma - X^3\Delta$ (0–0) systems. Fully coupled calculations by Schwenke (1998) predicted that these bands could contribute in the analysed spectral region.⁴ None of these systems, however, has yet been observed experimentally. Because *ab initio* calculations provide only approximate band positions, some flexibility existed in assigning the observed lines to these transitions. Indeed, the fitted lower-state spectroscopic constants were also consistent with the $X^3\Delta_3$ state (Ram et al. 1999). A counterargument was that, if the band belonged to the $D^3\Sigma^- - X^3\Delta$ or $h^1\Sigma - X^3\Delta$ systems, a stronger contribution from the $X^3\Delta_2$ spin component would be expected in the lower state.

The hypothesis that the lower state of the band is the ground $X^3\Delta$ state can also be tested using astrophysical observations alone. Because the proposed transition would originate from the ground state and overlaps with the $C^3\Delta - X^3\Delta$ band arising from the excited vibrational level ($v=3$), their relative contributions to opacity should differ in environments with enhanced columns of cold absorbing gas. Such conditions were present in the red nova V838 Mon shortly after its 2002 eruption, when large column densities of molecular gas at temperatures of 200–300 K were observed along the line of sight (Kamiński et al. 2009). Although a strong velocity gradient in the outflow smeared out de-

tailed band structure, we estimated the column density of gas in the ($v=3$) level of the ground state by fitting the γ (2–3) band in the near-infrared. The same column density was then used to synthesize the $C^3\Delta - X^3\Delta$ (1–3) band. This purely observational test showed that the band contour is insensitive to the presence of large columns of cold gas, effectively ruling out the ground $X^3\Delta$ state as the lower level of the analysed band.

With the firm identification of $a^1\Delta$ ($v=0$), as the lower state, these earlier considerations are no longer required. Nevertheless, the question of the non-detection of the predicted $D^3\Sigma^- - X^3\Delta$ and $h^1\Sigma - X^3\Delta$ systems remains open.

5. Conclusions

The identification of the $i^1\Pi - a^1\Delta$ band in stellar spectra has long been obscured because it overlaps with the much stronger $C^3\Delta - X^3\Delta$ (1–3) band and because the lower levels of the two transitions have similar energies ($a^1\Delta$, ($v=0$): 3444 cm $^{-1}$; $X^3\Delta$, ($v=3$): 2973 cm $^{-1}$; Ram et al. 1999). As a result, over the wide temperature range encountered in stars of different spectral types, the populations of these lower levels vary in a similar way, preserving the overall contour and masking the presence of the weaker system.

Line intensities of TiO electronic systems may differ by up to an order of magnitude, as can be seen from comparisons of the γ' ($B^3\Pi - X^3\Delta$) system in the line lists of Schwenke (1998), Plez (1998), and McKemmish et al. (2017). Even smaller discrepancies in other systems can produce noticeable differences in synthetic spectra (Jones et al. 2023), and substantial variations are expected between grids of late-type stellar models computed with different TiO line lists (Allard et al. 2000). Observed mismatches in TiO band strengths often encourage empirical adjustments to band intensities in order to reproduce stellar spectra. Within a single electronic system, relative band intensities are partly constrained by laboratory analyses, for example through reconstruction of potential energy curves from vibrational data. Residual discrepancies may be attributed to inaccuracies in *ab initio* transition dipole moment functions, which is not unexpected. In the present case, we encountered a similar issue for the ($\Delta v=-2$) sequence of the α system; however, the solution proved different. The discrepancies were instead caused by the presence of a previously unassigned electronic system. This discovery demonstrates that empirical determinations of band strengths remain uncertain until all significant opacity sources are identified.

Several TiO systems in the visual spectral range are still poorly characterized, both in line positions and intensities. Ex-

⁴ The NASA AMES TiO line list was distributed for stellar atmosphere calculations on Kurucz CD-ROM No. 24 (Kurucz 1999).

amples include the triplet $D^3\Sigma^- - X^3\Delta$ and the forbidden $h^1\Sigma - X^3\Delta$ systems. Forbidden bands of $c^1\Phi - X^3\Delta$ and $b^1\Pi - X^3\Delta$ were identified by Kamiński et al. (2009) in the spectrum of the red nova V838 Mon, where enhanced column densities of cool gas made their detection possible. Notably, the band heads of the $c^1\Phi - X^3\Delta$ system had already been reported as unidentified features in Mira spectra by Merrill et al. (1962). Although laboratory measurements provide accurate line positions for these bands, their intensities are currently based only on theoretical calculations (Schwenke 1998) and require experimental verification (Kamiński et al. 2009).

Weak, previously unidentified TiO systems likely contribute only modestly to the total opacity but can provide additional absorption in spaces between rotational lines of stronger overlapping bands lowering effectively the level of continuum, an effect that is particularly evident in spectral synthesis of high-resolution. In this respect, such systems play a role similar to that of minor TiO isotopologues (Jørgensen 1994).

A systematic approach combining high-resolution, high signal-to-noise stellar spectra with detailed laboratory analyses can therefore aid in identifying yet unobserved TiO systems and in reducing discrepancies between observed and synthetic spectra. This is an essential step toward more reliable determinations of stellar parameters and chemical abundances in M-type stars.

Acknowledgements. I gratefully acknowledge the memory of my late colleague Dr Yákov Pavlenko, whose collaboration inspired me to continue research on molecular bands in stellar spectra. I also thank Dr. Tomasz Kamiński for his financial support of M.S.'s participation in the ExoMol workshop funded by Grant SONATA BIS No. 2018/30/E/ST9/00398 from the Polish National Science Center, and for his patient attention to the early, albeit erroneous, hypotheses on the origin of the molecular band analysed here.

References

Allard, F., Hauschildt, P. H., & Schwenke, D. 2000, *ApJ*, 540, 1005
 Barnes, M., Merer, A. J., & Metha, G. F. 1997, *Journal of Molecular Spectroscopy*, 181, 180
 Bernath, P. 2020, *ApJ*, 895, 87
 Bernath, P. & Cameron, W. D. 2020, *ApJ*, 904, 24
 Bernath, P. F., Bhusal, M., & Schmidt, M. R. 2025, *ApJ*, 987, 126
 Bittner, D. M. & Bernath, P. F. 2018, *ApJS*, 236, 46
 Cameron, W. D. & Bernath, P. 2022, *ApJ*, 926, 39
 Dobrodey, N. V. 2001, *A&A*, 365, 642
 Fowler, A. 1904, *Proceedings of the Royal Society of London Series I*, 73, 219
 Gustafsson, B., Edvardsson, B., Eriksson, K., et al. 2008, *A&A*, 486, 951
 Hodges, J. N. & Bernath, P. F. 2018, *ApJ*, 863, 36
 Jones, H. R. A., Pavlenko, Y., Lyubchik, Y., et al. 2023, *MNRAS*, 523, 1297
 Jørgensen, U. G. 1994, *A&A*, 284, 179
 Kaledin, L. A., Mccord, J. E., & Heaven, M. C. 1995, *Journal of Molecular Spectroscopy*, 173, 499
 Kamiński, T., Schmidt, M., Hajduk, M., et al. 2023, *A&A*, 672, A196
 Kamiński, T., Schmidt, M., Tylenda, R., Konacki, M., & Gromadzki, M. 2009, *ApJS*, 182, 33
 Kurucz, R. 1999, *Robert Kurucz CD-ROM*, 24
 Langhoff, S. R. 1997, *ApJ*, 481, 1007
 Lefebvre-Brion, H. & Field, R. W. 1985, *Perturbations in the spectra of diatomic molecules* (Academic Press Inc., Orlando, FL)
 McKemmish, L. K., Masseron, T., Hoeijmakers, H. J., et al. 2019, *MNRAS*, 488, 2836
 McKemmish, L. K., Masseron, T., Sheppard, S., et al. 2017, *ApJS*, 228, 15
 Merer, A. J. 1989, *Annual Review of Physical Chemistry*, 40, 407
 Merer, A. J., Huang, G., Cheung, A. S.-C., & Taylor, A. W. 1987, *Journal of Molecular Spectroscopy*, 125, 465
 Merrill, P. W., Deutsch, A. J., & Keenan, P. C. 1962, *ApJ*, 136, 21
 Miliordos, E. & Mavridis, A. 2010, *The Journal of Physical Chemistry A*, 114, 8536, pMID: 20113002
 Namiki, K.-i. C., Ito, H., & Davis, S. P. 2003, *Journal of Molecular Spectroscopy*, 217, 173
 Phillips, J. G. 1973, *ApJS*, 26, 313
 Plez, B. 1998, *A&A*, 337, 495
 Ram, R. S., Bernath, P. F., Dulick, M., & Wallace, L. 1999, *ApJS*, 122, 331
 Raskin, G., van Winckel, H., Hensberge, H., et al. 2011, *A&A*, 526, A69
 Royer, P., Merle, T., Dsilva, K., et al. 2024, *A&A*, 681, A107
 Schwenke, D. W. 1998, *Faraday Discussions*, 109, 321
 Tennyson, J., Yurchenko, S. N., Zhang, J., et al. 2024, *J. Quant. Spectr. Rad. Transf.*, 326, 109083
 Tylenda, R., Kamiński, T., & Schmidt, M. 2009, *A&A*, 503, 899
 Western, C. M. 2017, *J. Quant. Spectr. Rad. Transf.*, 186, 221
 Woodward, C. E., Pavlenko, Y. V., Evans, A., et al. 2020, *AJ*, 159, 231
 Yurchenko, S. N., Lodi, L., Tennyson, J., & Stolyarov, A. V. 2016, *Computer Physics Communications*, 202, 262